

## BIOSORPTION OF FURFURAL AND MERCURY FROM AQUEOUS SOLUTION BY ANAEROBIC SLUDGE LIVE AND DEAD BIOMASS IN BATCH SYSTEM

ABBAS H. SULAYMON<sup>1</sup> & HAYFA'A L. SWADI<sup>2</sup>

<sup>1</sup>Department of Power Engineering, Baghdad University, Baghdad, Iraq

<sup>2</sup>Department of Chemical Engineering, Basrah University, Basrah, Iraq

### ABSTRACT

The biosorption of furfural and  $\text{Hg}^{2+}$  from simulated waste water using anaerobic sludge live and dead biomass were investigated. Batch type experiments were carried out to find the equilibrium isotherm data for each single and binary system. Ten isotherm models were used for single component and four models for binary system. Langmuir model gave the best fitting for the single system, while the binary system was fitted successfully with extended Langmuir model. The biosorption capacity for single system decreased by 18-47 % and 53-88 % in the binary system. Species of microorganisms identified in anaerobic sludge. The microorganisms found in the sludge were heterogeneous and consist mainly from facultative anaerobic bacteria, yeast, fungi and protozoa. FT-IR analysis was carried out before and after biosorption to determine which functional groups were responsible for binding the heavy metals and furfural.  $R^2$  used to enhance the justification analysis for each used model.

**KEYWORDS:** Biosorption, Anaerobic Sludge, Furfural,  $\text{Hg}^{2+}$ , Langmuir Model

### INTRODUCTION

Mercury is generally considered to be one of the most toxic metals found in the environment [1, 2]. The major sources of mercury pollution in the aquatic environment are industries such as chloralkali, paint, pulp, oil refining, electrical, rubber processing and fertilizer [3]. Mercury causes damage of the central nervous system and chromosomes, impairment of pulmonary function and kidneys, chest pain and dyspnea. Hence it is essential to remove mercury from wastewaters before its transport and cycling into the environment [4]. While furfural is organic compound that enter the aquatic environment through direct discharge from oil refineries. The content of the pollutant in the industrial wastewater are usually higher than the standard limit (less than 5 ppm for furfural compound. Direct contact with this substance should be avoided since this substance causes sensitivity of the skin, eye, mucous membranes, even the destruction of the liver, kidney and osteoporosis [5]. Various types of technology are available for removing furfural and mercury from water and wastewater. These include chemical precipitation, conventional coagulation, lime softening, reverse osmosis, ion-exchange and activated carbon adsorption [6]. The use of biological materials for heavy metal removal and recovery technologies has gained high credibility during recent years, due to high-quality performance and low cost of the materials.

Biosorption can be defined as the ability of biological materials to accumulate heavy metals from wastewater through metabolically mediated or physico-chemical pathways of uptake [7]. The term biosorption is used to describe the pollutant removal by both live and dead biomass (biosorbent). However; to be precise, bioaccumulation can be defined as the uptake of toxicants by living cells. The toxicant can transport into the cell, accumulate intracellularly, across the cell

membrane and through the cell metabolic cycle [8]. Conversely, biosorption can be defined as the passive uptake of toxicants by dead/inactive biological materials or by materials derived from biological sources. Biosorption is due to a number of metabolism-independent processes that essentially take place in the cell wall, where the mechanisms responsible for the pollutant uptake will differ according to the biosorbent type. Biosorption possesses certain inherent advantages over bioaccumulation processes. In general, the use of living organisms may not be an option for the continuous treatment of highly toxic organic/inorganic contaminants. Once the toxicant concentration becomes too high or the process operated for a long time, the amount of toxicant accumulated will reach saturation. Beyond this point, an organism's metabolism may be interrupted, resulting in death of the organism. This scenario can be biosorption is generally used for the treatment of heavy metal pollutants in wastewater. Application of biosorption for organic and other pollutants could also be used for the treatment of wastewater [9].

The aim of this study was to investigate the sorption capacity, removal efficiency of toxic metal ion of mercury and organic compound furfural from simulated wastewater as single and binary system onto live anaerobic sludge (LAS) and granular dead anaerobic sludge (GDAS).

## MATERIALS AND METHODS

### Live Anaerobic Sludge (LAS)

The anaerobic sludge used in the present study was collected as slurry from sewage sludge collection system (Hamdan wastewater treatment station in Basrah city, Iraq). To identify species of microorganisms present in anaerobic sludge, the sludge was serially diluted with distilled water. A liquots (0.1 ml) are spread on different nutrients agar and cultivated in incubator (memmert , ICP 500, Germany) at 303 K for 3-7 days. The microorganisms found in the sludge were heterogeneous and consist mainly from facultative anaerobic bacteria, yeast, fungi and protozoa .Seeded nutrient medium (2000 mg/l NaCH<sub>3</sub>COO as the sole carbon source, 500 mg/l NH<sub>4</sub>NO<sub>3</sub>, 500 mg/l KH<sub>2</sub>PO<sub>4</sub>, 200 mg/l CaCl<sub>2</sub> and 200 mg/l MgSO<sub>4</sub>) is used for microorganism's growth before used in batch experiments [10].The species of microorganisms identified in anaerobic sludge were tabulated in Table 1.

**Table 1: Species of Microorganisms Identified in Anaerobic Sludge**

Species of Bacteria		CFU/ml	Gram-Positive	Gram-Negative
Pseudomonas aeruginosa		$3.5 \times 10^8$		-
Escherichia coli		$4.3 \times 10^8$		-
Bacillus subtilis		$2.4 \times 10^6$	+	
Proteus mirabilis		$5.0 \times 10^5$		-
Entrobacter cloacae		$3.0 \times 10^5$		-
Salmonella sp.		$20 \times 10^9$		-
Shigelladysenteria		$25 \times 10^9$		-
Staphylococcus xylosus		$1.36 \times 10^9$	+	
Aeromonascaviae		$2.22 \times 10^4$		-
Klebsiellapneumoniae		$4.30 \times 10^4$		-
Species of Yeast		CFU/ml	Species of Protozoa	Species of Fungi
Candida albicans	17200	Entamoeb		Penicilliumchrysogenum
		Guardiglabilig		
		Ova of worm		

### Biosorbent Granule Dead Anaerobic Sludge (GDAS)

Granule dead anaerobic sludge was used as a biosorbent in the present work. It was obtained from Hamdan wastewater treatment station in Basrah city, Iraq. The sludge was washed several times with distilled water to remove undesired solid materials and dissolved heavy metals, dried under sun light, then dried in oven at 60 °C until having constant weight (24 h). The dry sludge was crushed by jaw crusher and sieved by successive sieves, then kept in desiccators for use. The physical and chemical properties were listed in Table 2.

**Table 2: Physical and Chemical Properties of GDAS**

Physical Properties	GDAS	Chemical Properties	GDAS
Actual density, kg/m <sup>3</sup>	1740.7	PH	7.5
Apparent density, kg/m <sup>3</sup>	608.9	Ash content, (%)	13
Particle porosity	0.65	Cation Exchange	51.153
Bed porosity	0.45		
Particle size, mm			
Pore volume, cm <sup>3</sup> /g			

### Adsorbate

1000 mg/l of stock solution of Hg<sup>2+</sup> ion and furfural (Fu) prepared by dissolving, Hg(NO<sub>3</sub>)<sub>2</sub>·1/2H<sub>2</sub>O and furfural respectively in distilled water. A solution of ions concentration of 50 mg/l was prepared by dilution of stock solution. Chemicals were used analytical grade produced by Fluka and BDH.

### Methods

The biosorption of Hg<sup>2+</sup> ion and furfural decrease at low pH values because of competition for binding sites between ions and protons, while at pH higher than 6, solubility of metal complexes decreases sufficiently allowing precipitation, which may complicate the biosorption process. Therefore the optimum pH was found around 4 [11, 12]. So, pH was adjusted with the range of (4) for all single and binary systems by adding the 0.1N HNO<sub>3</sub> and 0.1N NaOH. For determination of equilibrium adsorption/ biosorption isotherm, a sample of (100 ml) of each solution is placed in bottles of (250 ml) in volume, containing (0.1, 0.2,...1.4 g) of GAC/GDAS. The bottles were then placed on a shaker and agitated continuously at 150 rpm and 303K for 6 h. After 6 h of agitation which was enough to reach equilibrium [13], the solution was filtrated using filter paper type (Wattmann no. 4) and a sample of (2 ml) was taken for analysis. An ion concentration in the supernatant was measured using atomic absorption spectrophotometer (model VGP-210 Buck scientific for mercury metals, while for furfural (model UV PD-303) spectrophotometer, and computed from the calibration curves.

The functional groups of GDAS were detected by FT-IR analysis before and after biosorption. The proportion of GDAS biomass/KBr was 1/100. The background was obtained from the scan of pure KBr. JASCO FTIR 4200 spectrum system was used for FT-IR analysis of GDAS. The adsorbed amount was calculated using the following mass balance equation:

$$q_e = (V_i C_0 - V_f C_e) / W \quad (1)$$

The performance of GDAS adsorption was evaluated in terms of its removal efficiency as RE (%).

$$RE \% = (C_0 - C_e) / C_0 \times 100 \quad (2)$$

## RESULTS AND DISCUSSIONS

### Single System

The biosorption isotherms were obtained by plotting the weight of the solute adsorbed per unit weight of (LAS) / (GDAS) ( $q_e$ ) against the equilibrium concentration of the solute in the solution ( $C_e$ ) at constant temperature [14]. For a single component systems of  $Hg^{2+}$  and furfural, the equilibrium isotherms were conducted at (303 K) with initial concentration of each component,  $C_0=50$  mg/l. These isotherms are shown in Figure (1 and 2). Ten isotherm models were used to fit the experimental data. Isotherm models were given in Table 3.

The parameters were evaluated by non-linear curve fitting method using STATISTICA version-16 and EXCEL-2007 software. Table 3 represents the parameters of each model, the correlation coefficients ( $R^2$ ) and the percentage reduction of adsorption/biosorption. It is clear from Figure (1 and 2) and Table 3 that the equilibrium isotherm for each single component is of favorable type, since  $0 < R_s < 1$  ( $R_s = 0.1704, 0.1879$ ) for furfural and  $Hg^{2+}$  onto LAS, while ( $R_s = 0.2732$ , and  $0.1372$ ) for furfural and  $Hg^{2+}$  onto GDAS respectively. The experimental data for mercury, where described successfully with Langmuir model with correlation coefficient 0.9938 and, 0.9938 onto LAS 0.9959 and 0.9922 onto GDAS respectively. It was found that the maximum metal uptake  $q_m$  (mg/g) for Fu is greater than that for  $Hg^{2+}$  onto LAS ( $q_{m,Fu}=28.1869$  and  $q_{m,Hg^{2+}}=35.2857$ ) while it is opposite for GDAS ( $q_{m,Fu}=45.8234$  and  $q_{m,Hg^{2+}}=48.1370$ ) respectively.

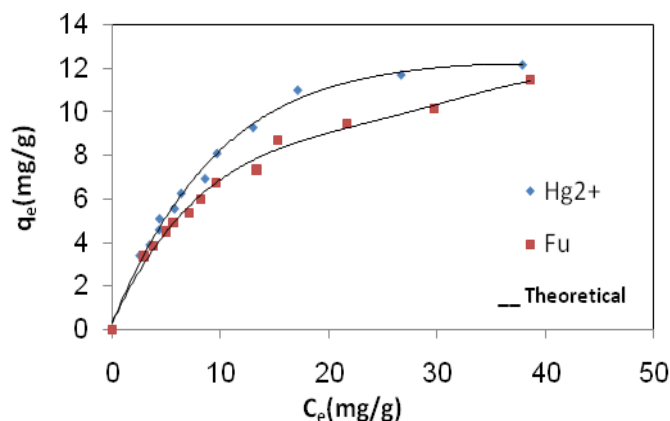


Figure 1: Biosorption Isotherm for Single Furfural and Mercury onto LAS at 303 K

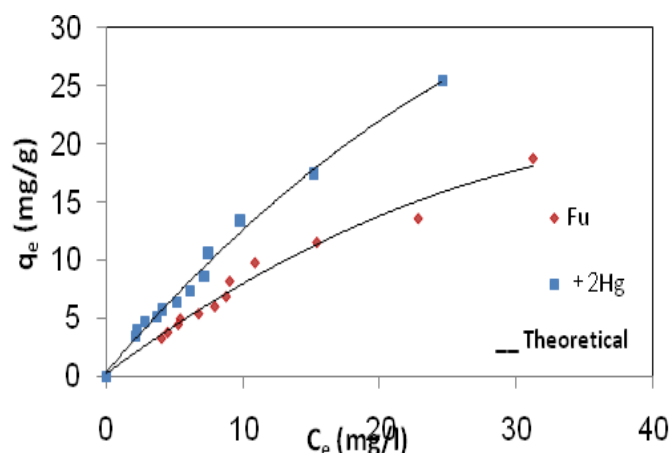


Figure 2: Biosorption Isotherm for Single Furfural and Mercury onto GDAS at 303 K

Table 3: Biosorption Isotherm Models and Parameters of Single Solute Isotherm for Fu and Hg<sup>2+</sup>

Model	Parameters	LAS		GDAS	
		Fu	Hg <sup>2+</sup>	Fu	Hg <sup>2+</sup>
Freundlich[15] $q_e = KC_e^{1/n}$	K(mg/g)(l/mg) <sup>1/n</sup> n R <sup>2</sup>	1.6754 2.35163 0.9924	1.98217 2.2129 0.9871	1.7184 1.6483 0.9956	2.0332 2.3448 0.9750
Langmuir [16] $q_e = \frac{q_m b C_e}{1 + b C_e}$	q <sub>m</sub> (mg/g) b (l/mg) R <sup>2</sup> R <sub>s</sub> E <sub>ad</sub> . (%)	28.1869 0.0973 0.9938 0.1704 94.2601	35.2857 0.0864 0.9938 0.1879 94.4920	45.8234 0.0590 0.9959 0.2732 97.4403	48.1370 0.1249 0.9922 0.1372 97.5420
Toth[17] $q_e = \frac{K_t C_e}{(a_t + C_e)^{1/t}}$	K <sub>t</sub> (mg/g) a <sub>t</sub> t R <sup>2</sup>	3.2853 2.3481 1.6431 0.9953	40.9845 10.8016 0.9325 0.9943	5.8241 0.1068 2.5086 0.9956	262.5796 18.0189 0.6818 0.9922
Combination of Langmuir-Freundlich $q_e = \frac{b q_m C_e^{1/n}}{1 + b C_e^{1/n}}$	q <sub>m</sub> (mg/g) b (l/mg) <sup>1/n</sup> n R <sup>2</sup>	30.5132. 0.0941 1.7219 0.9958	19.8475 0.1136 1.1865 0.9945	103.3115 0.0417 1.3182 0.9959	157.6417 0.1243 0.9776 0.9907
Khan [19] $q_e = \frac{Q_{\max} b_k C_e}{(1 + b_k C_e)^{a_k}}$	Q <sub>max</sub> (mg/g) b <sub>k</sub> (l/mg) a <sub>k</sub> R <sup>2</sup>	1.8421 6.2315 0.5182 0.9952	51.1857 0.0643 1.5657 0.9921	2.0343 5.9081 0.4018 0.9956	52.4579 0.0563 1.45587 0.9922
Temkin(Temkin, 1934 )[20] $q_e = \frac{RT}{b} \ln(K_T C_e)$	B <sub>1</sub> (KJ/mole) K <sub>T</sub> (l/mg) R <sup>2</sup>	0.8427 1.0125 0.8924	0.4786 0.8292 0.9572	1.3642 0.9329 0.9047	0.9182 13.321 0.9481
BET [21] $q_e = \frac{BQC_e}{(C_s - C_e)[1 + (B-1)(C_e/C_s)]}$	B (l/mg) Q (mg/g) R <sup>2</sup>	1.5421*10 <sup>14</sup> ^14 8.8631	532.926 19.2157 0.78261	6.5724 34.1201 0.9776	167.2391 15.3876 0.7841
Harkins - Henderson [22] $q_e = \frac{K_h^{1/n_h}}{C_e^{1/n_h}}$	K <sub>h</sub> (mg/g)(mg/l) <sup>1/n<sub>h</sub></sup> n <sub>h</sub> R <sup>2</sup>	0.01153 -1.9587 0.9953	0.0053 -1.7629 0.9941	0.0143 -1.8436 0.9689	0.0096 -1.5986 0.9624
Redlich-Peterson[23] $q_e = \frac{A_R C_e}{1 + B_R C_e^{m_R}}$	A <sub>R</sub> (l/mg) B <sub>R</sub> (l/mg) <sup>m<sub>R</sub></sup> m <sub>R</sub> R <sup>2</sup>	8.3761 0.9568 0.6987 0.9956	0.3258 0.1762 1.1983 0.9928	11.7562 1.8432 6.14738 0.9942	0.5163 0.2841 1.2652 0.9927
Radke-Praunsitz[24] $q_e = \frac{K_{RP} C_e}{1 + (\frac{K_{RP}}{F_{RP}}) C_e^{1-N_{RP}}}$	K <sub>RP</sub> (l/mg) F <sub>RP</sub> N <sub>RP</sub> R <sup>2</sup>	2.1249 10.1317 0.7015 0.9946	0.7182 69.8716 -0.1934 0.9921	17. 2864 6.7329 0.7829 0.9959	0.5732 56.9483 0.0743 0.9931

### Fourier –Transform Infrared Analysis (FT-IR)

In order to find out which functional groups were responsible for the Fu and  $\text{Hg}^{2+}$  biosorption, FT-IR analysis of raw and loaded GDAS was carried out.

Infrared spectra of GDAS samples before and after furfural and mercury binding was shown in Figure 3 and listed in Tables 4. Spectra analysis of FT-IR spectrum after cations adsorption showed that there was a substantial decrease in the wave number and adsorption intensity of GDAS. The carboxylic acid, amide and alkyl halides groups at 3414, 2929.95 and 1652.88  $\text{cm}^{-1}$  are the major groups in biosorption process.

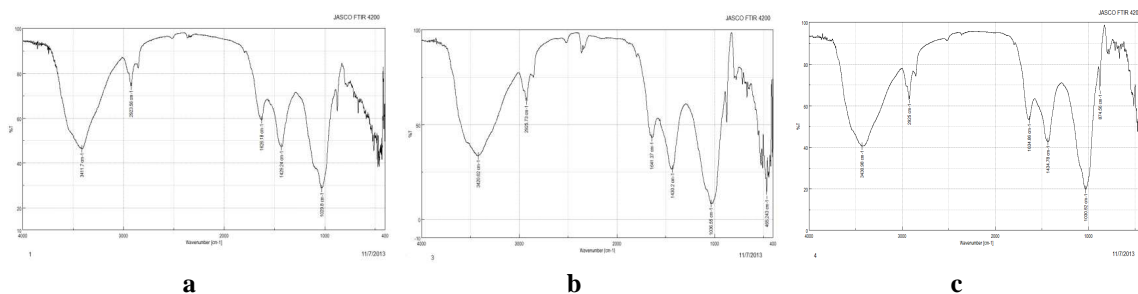


**Figure 3: FT-IR Analysis for Granular Dead Anaerobic Sludge (a) Raw GDAS, (b) Fu-Loaded GDAS and (c) Hg Loaded GDAS**

**Table 4: FT-IR Analysis for Raw and Loaded GDAS**

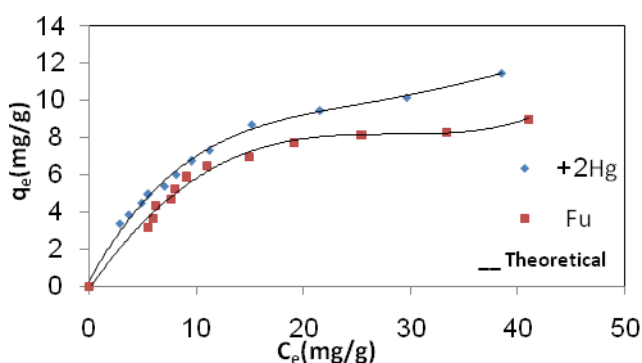
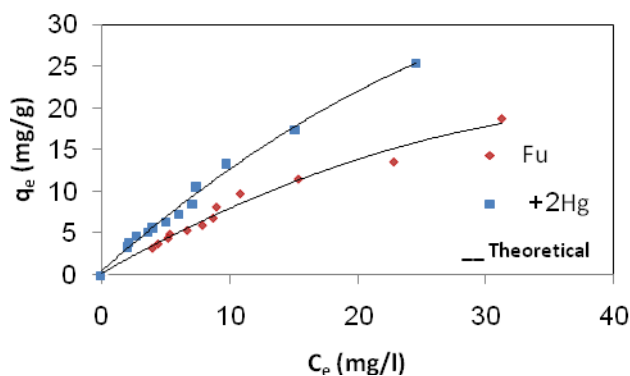
Wave Number, $\text{cm}^{-1}$	Type of Bond	Functional Group	Tr (%) before Biosorption	Tr (%) after Biosorption		Difference in Peaks Absorption %	
				Fu	$\text{Hg}^{2+}$	Fu	$\text{Hg}^{2+}$
3741.90	-OH <sup>-</sup>	Carboxylic acid	76	95	96	19	20
3549.02	-OH <sup>-</sup>	Carboxylic acid	36	66	63	30	27
3475.73	-OH <sup>-</sup> , -NH <sup>+</sup> , -NH <sub>2</sub> <sup>+</sup>	Carboxylic acid, Amide, Amine	28	60	58	32	30
3414.00	-OH <sup>-</sup> , -NH <sup>+</sup> , -NH <sub>2</sub> <sup>+</sup>	Carboxylic acid, Amide, Amine	25	57	57	32	32
2954.95	-OH	Carboxylic acid	51	72	74	21	23
2920.23	-CH <sup>+</sup>	Alkane	33	49	56.5	16	24
2850.79	-CH <sup>+</sup>	Alkane	47	66	67	19	20
2515.18	-OH <sup>-</sup>	Carboxylic acid	80	96	90	16	10
2360.87	-CH <sup>+</sup>	Alkane	80	93	103	13	23
1797.66	-C=O <sup>-</sup>	Carboxylic acid	75	93	97	18	22
1639.49	-CH <sup>+</sup>	Alkane	35	59	96	24	31
1562.34	-NH <sup>-</sup>	Amide	38	50	63	12	25
1419.61	-OH <sup>-</sup>	Carboxylic acid	28	41	58	13	30
1080.14	-C-O-C-	Alcohol	31	41	57	10	26
1029.99	-C-O-C-, OH-	Alcohol, Carboxylic acid	22	31	74	9	52
875.68	-CH <sup>+</sup>	Aromatic	50	75	56.5	25	6.5
797.24	-PH <sup>+</sup>	Phosphines	58	80	67	22	9
713.66	-C-Cl-	Alkyl halides	54	79	90	24	36
582.07	-C-I-	Alkyl halides	44	76	103	32	59

Table 4: Contd.,

513.07	-C-Br-	Alkyl halides	32	62	97	30	65
Sum of difference in peaks absorption %, (after – before) adsorption						420	570

### Binary System

For a binary system of  $\text{Hg}^{2+}$  and furfural the equilibrium isotherms were conducted at (303 K) with initial concentration of each component,  $C_0=50$  mg/l these isotherms were shown in Figure (4 & 5). Four isotherm models were used to fit the experimental data. The isotherm models are given in Table 5 which represents the values of the parameters of each used model and the correlation coefficients ( $R^2$ ). The behavior of the equilibrium isotherms for all the binary systems is of a favorable type. The extended Langmuir and Redlich-Peterson models to give the best fitting ( $R^2=0.9977$  and  $0.9981$ ) for the experimental data for furfural biosorption onto LAS. While onto GDAS the extended Langmuir model gave the highest value of ( $R^2=0.9973$ ). For mercury biosorbed onto LAS, the extended Langmuir and combination of Langmuir-Freundlich are the best fit models ( $R^2=0.9961$  and  $0.9962$ ). However, onto GDAS the extended Langmuir and Redlich-Peterson are the most fitting models ( $R^2=0.9962$  and  $0.9944$ ). From the figures and related tables,  $\text{Hg}^{2+}$  always adsorbed more favorably onto GDAS than Fu.

Figure 4: Biosorption Isotherm of (Fu - $\text{Hg}^{2+}$ ) onto LAS at 303 KFigure 5: Biosorption Isotherms for (Fu- $\text{Hg}^{2+}$ ) onto GDAS at 303 K

**Table 5: Biosorption Isotherm Models and Parameters of Binary Solute Isotherm for Fu and Hg<sup>2+</sup>**

Model	Parameters	LAS		GDAS	
		(Fu- Hg <sup>2+</sup> ) Solution		(Fu- Hg <sup>2+</sup> ) Solution	
		Fu	Hg <sup>2+</sup>	Fu	Hg <sup>2+</sup>
Extended Langmuir $[25] q_{e,i} = \frac{q_{m,i} b_i C_{e,i}}{1 + \sum_{k=1}^N b_k C_{e,k}}$	q <sub>m</sub> (mg/g)	5.7891	17.145	21.3756	36.6349
	b(l/mg)	0.1895	0.09891	0.0529	0.0830
	R <sup>2</sup>	0.9977	0.9961	0.9973	0.9962
	R <sub>s</sub>	0.0956	0.1682	0.2743	0.19142
	E <sub>bio.</sub> (%)	95.356	93.084	92.020	95.780
Combination of Langmuir-Freundlich[26] $q_{e,i} = \frac{q_{m,i} b_i C_{e,i}^{1/n_i}}{1 + \sum_{i=1}^N b_i C_{e,i}^{1/n_i}}$	q <sub>m</sub> (mg/g)	0.0276	15.5632	1.8709	6.7560
	b	98.7624	16.9672	4.8381	4.3793
	n	10.2153	3.9672	1.4916	0.0833
	R <sup>2</sup>	0.9688	0.9962	0.9877	0.9939
Redlich-Peterson [26] $q_{e,i} = \frac{K_{Ri} (b_{Ri}) C_{e,i}}{1 + \sum_{k=1}^N b_{R,k} (C_{e,k})^{m_{R,k}}}$	K <sub>R</sub> (l/mg)	3.7642	2.8896	1.4367	11.2354
	b <sub>R</sub> (l/mg) <sup>m<sub>R</sub></sup>	0.1647	14.2581	11.4763	13.7829
	m <sub>R</sub>	1.6940	0.9278	0.1004	0.7116
	R <sup>2</sup>	0.9981	0.9935	0.9962	0.9944
Extended Freundlich[27] $q_{e,i} = \frac{K_i C_{e,i}^{n_i+n_1}}{C_{e,i}^{n_1} + \sum_{j=1}^N K_j C_{e,j}^{n_j}}$	K (mg/g)(l/mg) <sup>1/n</sup>	0.03582	46.4591	7.3540	46.0430
	n	0.24769	0.9856	0.1159	0.6754
	R <sup>2</sup>	0.9864	0.9912	0.9895	0.9921

### Removal Efficiency

The removal efficiency of biosorption represents the ability of biosorbent to reduce or remove the adsorbates from the solution. The removal efficiency was calculated by using equation (2). The percentage removal was tabulated in (6). From this table the removal percentage achieved for highest mass of LAS/GDAS for the single and binary system for all pollutants. Hg<sup>2+</sup> gives the maximum percentage removal rather than Fu onto LAS/GDAS this may be due to the physical and chemical properties of Hg<sup>2+</sup> to be more favorable to be adsorbed than Fu. For binary system and for all pollutants there are reductions in the percentage of removal. This is due to the presence of more than one pollutant within the same adsorbent/biosorbent which will enhance the competition and the struggling race of each pollutant to occupy an adsorbent site and hence, an occupied site will be a mixture of two adsorbed species. Therefore reducing the percentage removal of the adsorbate as they are in their single state.



Table 6: Removal Efficiency for Each Pollutant

Weight (g)	Single				Binary			
	LAS RE%		GDAS RE%		LAS RE%		GDAS RE%	
	Fu	Hg <sup>2+</sup>	Fu	Hg <sup>2+</sup>	Fu	Hg <sup>2+</sup>	Fu	Hg <sup>2+</sup>
0.1	11.46	12.122	20.8	24.13	9	11.655	18.744	25.433
0.2	40.654	46.654	65.63	76.94	33.154	45.75	54.322	69.75
0.3	56.784	65.774	77.08	82.752	48.882	61.354	69.178	80.494
0.4	69.574	74.026	81.76	86.25	61.766	71.776	78.256	85.144
0.5	73.4	80.684	85.8	89.248	69.978	78.444	81.954	85.742
0.6	80.856	82.892	88.3	93.1	78.024	81.772	82.47	87.804
0.7	83.75	87.318	91.14	95.708	81.714	86.826	84.136	89.772
0.8	85.91	88.536	93.47	96.048	83.886	86.888	86.514	91.91
0.9	88.804	91.302	92.43	96.208	84.712	89.114	89.2	92.692
1	90.072	91.37	94.43	96.694	87.484	90.474	89.498	94.44
1.2	92.47	93.096	94.71	97.16	88.02	91.532	91.048	95.598
1.4	94.26	94.942	95.02	97.524	88.864	92.888	91.936	95.792

### Combination Component Systems

The biosorption isotherms for each solute in the combination systems (single and binary) were shown in Figure (6 to 9). From the figures when Fu and Hg<sup>2+</sup> are competing for the same type of adsorbent, pollutants with greater affinity (strongly adsorbed species) will displace others with a lower affinity (weakly adsorbed species). There is a weak competition in binary systems in the biosorption capacity of mercury onto LAS and GDAS respectively ( $\Delta q_{m,Hg^{2+}} = 18 \text{ mg/g}$  and  $12 \text{ mg/g}$ ), whereas the uptake of furfural is highly reduced by the presence of mercury solute due to higher affinity between mercury and biosorption sites ( $\Delta q_{m,Fu} = 22 \text{ mg/g}$  and  $24.5425 \text{ mg/g}$ ). GDAS is more efficient than LAS in biosorbed furfural and mercury because these pollutants could be toxicants to live microorganisms. In addition, some of these microorganisms considered to be pathogenic to human such as *Klebsiella pneumonia*.

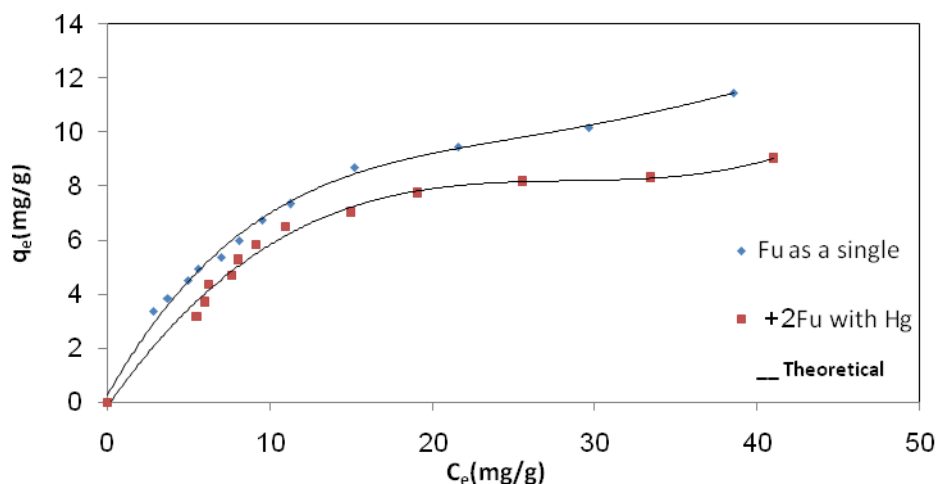


Figure 6: Biosorption Isotherms for Furfural onto LAS in Single and Binary Systems at 303 K

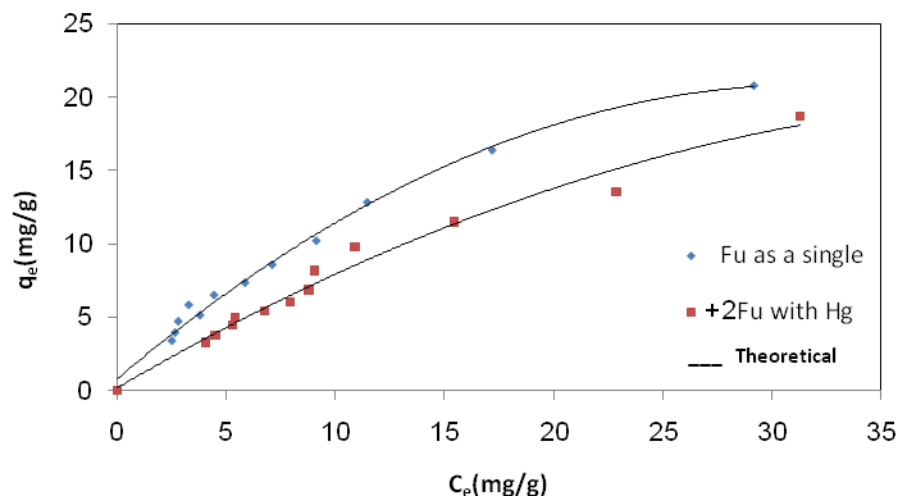


Figure 7: Biosorption Isotherm for Single and Binary System for Furfural onto GDAS at 303 K

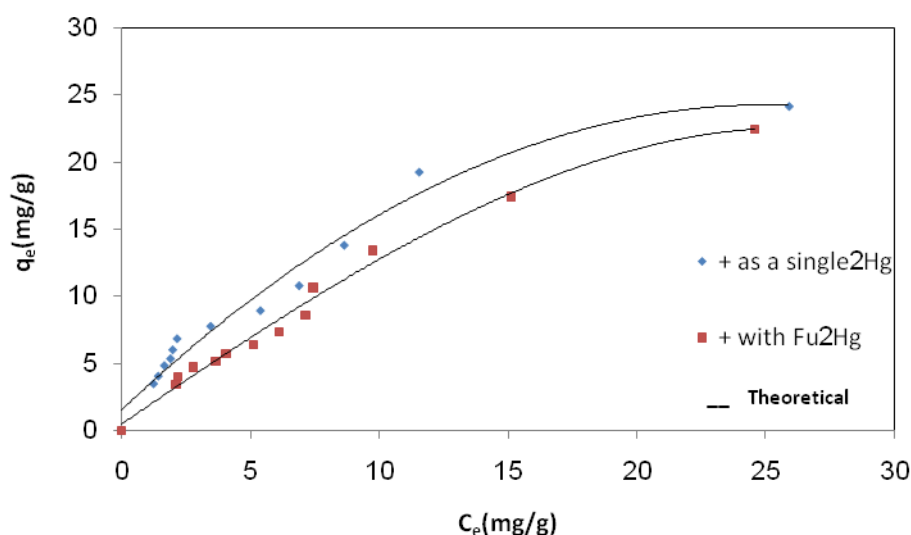


Figure 8: Biosorption Isotherm for Single and Binary System for Mercury onto GDAS at 303 K

### Comparisons between Biosorption Capacities

The comparison between biosorption capacity for furfural and  $\text{Hg}^{2+}$  onto LAS and GDAS in single system is shown in Figure (9). The use of GDAS offers several advantages over LAS the pollutants removal system is not subject to toxicity limitations, there is no requirement for growth media and nutrients, the biosorbed pollutants can be easily desorbed and biosorbents can be reused. Table 7 summarized the comparison between biosorption by LAS and GDAS for the experiments achieved in batch system.

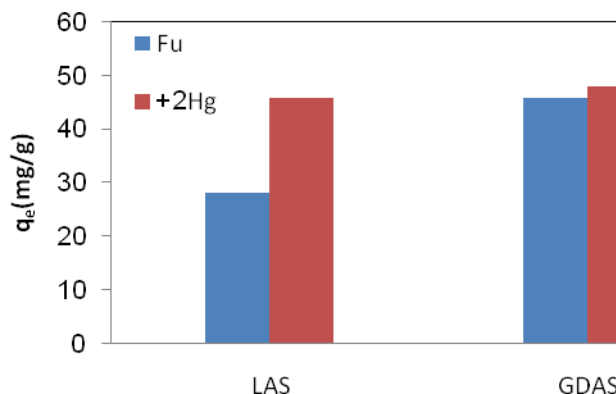


Figure 9: Furfural and Mercury Biosorption onto LAS/GDAS in Single System

Table 7: Comparison between Biosorption by LAS and GDAS

Property		Furfural Biosorption		Mercury Biosorption	
		LAS	GDAS	LAS	GDAS
Maximum uptake, $q_m$ (mg/g)		28.1869	45.8235	35.2857	48.1373
Isotherm Model	single	L,C	L, C	L,C	L, C
	binary	EL,R-P	EL, R-P	EL	EL, C
Mechanisms of biosorption	Physical	Major effect	Major effect	Major effect	Major effect
	Ion exchange	Non	51.153 meq/100 g	Non	51.153 meq/100 g
	Chemical	Minor effect	Minor effect	Minor effect	Minor effect
Sum of difference in peaks absorption %, (after - before) adsorption		Non	420	Non	570

L=Langmuir model, C= Combination of Langmuir-Freundlich model, EL=Extended Langmuir model, R-P=Redlich-Peterson.

## CONCLUSIONS

Based upon the experimental results and theoretical application models in batch systems, the results showed:

- GDAS was more efficient than LAS in biosorption of furfural and mercury.
- Functional groups of GDAS responsible for biosorption for mercury exceed that for furfural.
- The equilibrium isotherm for each component Fu and  $Hg^{2+}$  onto LAS /GDAS were of favorable type. In addition to the familiar Langmuir model. While for binary system, extended Langmuir model was well fitted the equilibrium isotherms.
- The biosorption capacity in single and binary (Fu and  $Hg^{2+}$ ) systems onto LAS /GDAS is:  $Hg^{2+} > Fu$  onto LAS /GDAS. This difference in behavior due to high affinity between  $Hg^{2+}$  LAS /GDAS.

## REFERENCES

- M.Yardim, Budinova, T. E. Ekinici and N. Petrov (2003) Removal of mercury (II) from aqueous solution by activated carbon obtained from furfural. Chemosphere, 52, 835-841.

2. J. Choong and K.H. Park (2005) Adsorption and desorption characteristics of mercury (II) ions using aminated chitosan bead. *Water Res.*, 39 3938-3944.
3. D.Manohar, K. Krishnanand T. Anirudhan (2002) Removal of mercury (II) from aqueous solutions and chloralkali industry wastewater using mercaptobenzimidazole clay. *Water Res.*, 36 1609-1619.
4. Y.Kacar, C. Arpa, S. Tan, A. Denizli, O.Genc, and M. Arica (2002) Biosorption of Hg (II) and Cd (II) from aqueous solutions: Comparison of biosorptive capacity of alginate and immobilized live and heat inactivated *Phanerocheatechrysosporium*. *Process. Biochem.*, 37601-610.
5. H. Hooshi, N. A. Ghotli, A. Sooki, S. Abbasi (2012) Using activated sludge system to reduce furfural concentration in A refinery wastewater. *Advances in Environmental Biology*, 6(8) 2378-2383.
6. P. Cyr, P. Suri, and E.Helmig (2002) A Pilot Scale evaluation of removal of mercury from pharmaceutical wastewater using granular activated carbon. *Water Res.*, (36) 4725-4734.
7. G.Naja, C.Mustin, B. Volesky and J. Berthelin (2006) Stabilization of the initial electrochemical potential for a metal-based potentiometric titration study of a biosorption process", *Chemosphere Vol. 62*, 1pp. 163-170.
8. A.Malik (2004) Metal bioremediation through growing cells, *Environ. Int.*, Vol. 30, pp.261–78.
9. M .Tsezosand J.P Bell (1989) Comparison of the biosorption and desorption of hazardous organic pollutants by live and dead biomass, *Water Res.*, Vol.23, p.23.
10. D.Tilaki, and R.Ali (2003)Study on removal of cadmium from water environment by adsorption on GAC, BAC and biofilter, *Env. Health Eng. Department, Faculty of Health, Mazandaran University of Medical Science*.
11. S.Tunali, A. Cabuk, and T. Akar (2006) Removal of lead and copper ions from aqueous solutions by bacterial strain isolated from soil. *Chem.Eng. J.*, 115, 203-11.
12. J.Farah, N. El-Gendy, and A. Farahat (2007)Biosorption of astrazone blue basic dye from an aqueous solution using dried biomass of Baker's yeast. *J. Hazard Mater*, 148, 402-408.
13. A. AjayKumar, A. Naif, and N. Hilal, (2009) Study of Various Parameters in the Biosorption of Heavy Metals on Activated Sludge, *World Applied Sciences Journal 5 (Special Issue for Environment)*, pp. 32-40.
14. J.C.Crittenden (1987) Evaluation multicomponent competitive adsorption in fixed-bed, *J. Environmental Engineering*, vol.113, No.6, pp.1363-1375.
15. H.Freundlich (1907) Ueberdie adsorption in loesungen. *Z. Phys. Chem.*, 57, 385-470.
16. G. Belfort (1980), Adsorption on carbon: theoretical considerations. *Environmental Science and Technology*,, 14(8), 910-913.
17. J. Toth (1971) State equations of the solid gas interface layer. *Acta. Chem. Acad. Hung*, 69,
18. R. Sips, On the structure of a catalyst surface. *J. Chem. Phys.*, 16(1984), 490-495.
19. A. Khan, T. Al-Bahri, and A. Al-Haddad (1997) Adsorption of phenol based organic pollutants on activated carbon from multi-component dilute aqueous solutions. *Water Res.*, 31, 2102-2112.

20. M. Temkin (1934) Die gas adsorption und der nernstschewärmesatz. Acta.Physicochem.URSS, 1, 36-52.
21. S. Brunauer,P. Emmet, E. Teller(1938), Journal of Chemical, , 60,309-319.
22. W.D Harkins, S Henderson (1952) Journal of Agriculture Engineering, 33 29-4.
23. O. Redlich; D.L. Peterson (1959) Journal of Physical and Chemical, 63, 1024-1025.
24. W. D. Harkins, and S. Henderson (1952)A basic concept of equilibrium moisture Agriculture Eng. J., 33, 29-41.
25. J. R.Weber and J.Walt (1979) Physicochemical Processes for Water Quality Control. New York: Wiley-Interscience.
26. Fahmi, K. Munther (2003) Separation Science and Technology, 38, 483-497.
27. F. Pagnanelli, M. Trifoni ,F .Beolchini, A. Esposito, L. Toro, F. Veglio (2001) Journal of Process Biochemistry, Vol. 37, pp. 115–124.

## NOMENCLATURE

**Table 8**

Symbol	Description	Units
A	Elovich model parameter	mg/g.s
$a_K$	Khan model parameter	-
$a_t$	Toth model parameter	-
$A_R$	Reddlich-Peterson model parameter	l/mg
B	BET model parameter	l/mg
$B_1$	Temkin isotherm constant,	kJ/gm
$b_K$	Khan model parameter	l/mg
C	Parameter in intra-particle diffusion model	mg/g
$C_e$	Equilibrium concentration	mg/l
$C_{ei}$	Equilibrium concentration of component i	mg/l
$C_0$	Initial solute concentration	mg/l
$F_{RP}$	Radke-Praunsitz model parameter	-
K	Freundlich equilibrium parameter	$(\text{mg/g})(\text{l/mg})^{1/n}$
$K_h$	Harkins-Henderson model parameter,	$(\text{mg/g})^n (\text{mg/l})$
$K_R$	Reddlich-Peterson model parameter(binary system)	l/mg
$K_{RP}$	Radke- Praunsitz model parameter	l/g
$K_T$	Equilibrium binding constant in Temkin model	l/mg
$m_R$	Reddlich-Peterson model parameter	
n	Freundlich equilibrium parameter and Sips model parameter	
$n_h$	Harkins-Henderson model parameter	
$N_{RP}$	Radke-Praunsitz model parameter	
Q	BET model parameter	mg/g
$Q_{\max}$	Khan model parameter	mg/g
$q_e$	Internal concentration of solute in particle at equilibrium	mg/g
$q_{ei}$	Amount of adsorbate adsorbed per mass of adsorbent of species i	$\text{g} \cdot \text{gm}^{-1} \cdot \text{min}^{-1}$
$q_m$	Adsorption capacity defined by Langmuir equation	mg/g

Table 8: Contd.,		
$q_{mi}$	Adsorption capacity for species i	
R	Universal gas constant	8.314 kJ/mol.K
$R_s$	separation factor	
T	Absolute temperature	K
t	Toth model parameter	
$V_f$	Final Volume of solution	ml
$V_i$	Initial Volume of solution	ml
W	Mass of granular activated carbon /granular dead anaerobic sludge	g